Materials Research Proceedings 37 (2023) 313-316 https://doi.org/10.21741/9781644902813-68

Adaptive finite elements based on Carrera unified formulation for meshes with arbitrary polygons

Maria Cinefra[1,a *] and Andrea Rubino[1,b]

[1]Politecnico di Bari, via Edoardo Orabona 4, Bari, Italy

[a]maria.cinefra@poliba.it, [b]andrea.rubino@poliba.it

Keywords: Carrera Unified Formulation, Adaptive Finite Elements, 3D Elements, Node-Dependent Kinematics, Arbitrary Polygons

Abstract. The new Adaptive Finite Elements presented are based on Carrera Unified Formulation (CUF) that permits to implement 1D and 2D elements with 3D capabilities. In particular, by exploiting the node-dependent kinematic approach recently introduced and incorporating the FEM shape functions with the CUF kinematic assumptions in unique 3D approximating functions, it is demonstrated that new mesh capabilities can be obtained with the use of presented elements by easy implementation. A classical patch test is performed to investigate the mesh distortion sensitivity.

Introduction

To alleviate meshing issues due to FEM, more advanced techniques can be used, resorting to numerical methods that are designed from the very beginning to provide arbitrary order of accuracy on more generally shaped elements. These techniques are based, for instance, on the Virtual Element Method (VEM) [1]. In fact, in contrast to FEM in which elements are typically triangular and quadrilateral in 2D or tetrahedral and hexahedral in 3D, the VEM permits arbitrary two-dimensional polygonal and three-dimensional polyhedral elements [2]. This allows the problem domain to be discretized by elements represented by arbitrary polygons, which can be concave and convex. Moreover, different polynomial consistency is allowed within the method and non-conforming discretizations can be handled, mainly for local refinement and so on, representing the key aspect of this method.

The newly proposed Adaptive Elements, which are Finite Elements based on Carrera Unified Formulation (CUF), represent more agile and manageable elements, based on a well-known technique (FEM), easy to implement and can produce the same benefits of using VEM. Recently, in the framework of CUF, a novel approach called Node-Dependent Kinematics (NDK) has been proposed to further increase the numerical efficiency of the models [3]. The Node-Dependent Kinematics approach, along with the 3D modelling of non-orthogonal geometries [4], opens the possibility to create elements with a non-conventional number of nodes, complex geometrical shapes, and different polynomial approximations along different spatial directions, leading to a certain freedom in modelling the problem considered. In this way, 3D elements can be recovered with a non-regular shape that can adapt to the edges of the domain considered, when the geometrical constraints or the kinematic behavior of the structure requires that.

Adaptive Finite Elements

In traditional beam and plate theories, it is difficult to model beams with variable sections or sections that are not orthogonal to the axis, as well as plates with varying thickness or edges not perpendicular to the mid-surface. However, with the Node-Dependent Kinematic approach [3], it is possible to extend the Carrera Unified Formulation models to incorporate more complex geometries. This is achieved by incorporating the CUF kinematic assumption with the FEM discretization to create a unique 3D approximation, as follows:

$$\mathbf{u} = (F_\tau^i N_i)\mathbf{q}_{\tau i} = L_{\tau i}(\xi, \eta, \zeta)\mathbf{q}_{\tau i}$$

Where where ξ, η, ζ are the natural coordinates corresponding to x, y, z and **u** = {u_x, u_y, u_z} is the 3D displacement field. A double summation over the indeces i=1,…, N_n and τ=1,…,M is implied, where N_n is the number of the nodes in the element and M is the number of approximating functions adopted for the kinematic theory. F_τ and N_i are defined according to the type of element (beam or plate): N_i are the FEM shape functions that are used along the axis for beam elements or in the plane for the plate elements; F_τ are the approximating functions over the cross-section for the beam or along the thickness for the plate. Lagrange polynomials are chosen in this work for generating both F_τ and N_i, according to the CUF [4]. $q_{\tau i}$ are the generalized nodal displacements. Note that the function F_τ depends on the node 'i'.

The function $L_{\tau i}$ = ($F^i_\tau N_i$) represents a non-conventional 3D shape function in which the order of expansion can be different along one of the spatial directions. As a result, this approach overcomes the limitations of classical 3D finite element, related to its aspect ratio, with a consequent saving in degrees of freedom and the possibility to create polygonal elements.

In the following, the acronyms B2 (linear), B3 (quadratic) and B4 (cubic) are used both for the 1D discretization of the axis in beam models or for the approximation through the thickness in plate models; as well as the acronyms Q4 (linear), Q9 (quadratic) and Q16 (cubic) are used both for the 2D approximation of the cross-section in beam models and for the discretization of the in-plane domain in plate models.

Patch test

This standard test is classically used in order to investigate the mesh distortion sensitivity in plate bending problems. The in-plane dimensions of the square plate considered are 100×100 m^2 and the thickness is 5 m. The boundary conditions are clamped (CC). A transverse concentrated force is applied at the center of the top surface F = 4 N. The material is isotropic with the following properties: E = 10.92 Pa, ν = 0.30 and ρ = 1 kg/m^3. The meshes initially used are a 4x4 Q4 elements and a 4x4 Q9 elements in the plane, with B3 approximation along the thickness in both cases.

Due to the symmetry of the problem, a quarter of the plate is considered. In particular, the bottom-left quarter of the plate is chosen and symmetry boundary conditions are applied along cut edges. F = 1 N is applied on the top-right corner. The resulting mesh of the plate quarter is 2 × 2 based on Q4 or Q9 plate elements.

Some beam elements are introduced in the mesh in order to obtain distorted elements with different number of nodes along the edges. Then, three different configurations are analyzed:

- 2xQ4 1xB2: in this configuration, the previous two elements at the top are substituted by a single 1D element with 2 nodes, having a Q9 approximation on the cross-section;
- 2xQ4 1xB3: as in the previous case, the two elements at the top are substituted by a single 1D element but having 3 nodes along the axis, where the cross-section is expressed as a Q9 element;
- 2xQ4 1xQ9: the number of nodes is identical with respect to the previous case, but the discretization of the two elements at the top is different, accounting for a single Q9 element having a B3 discretization along the thickness.

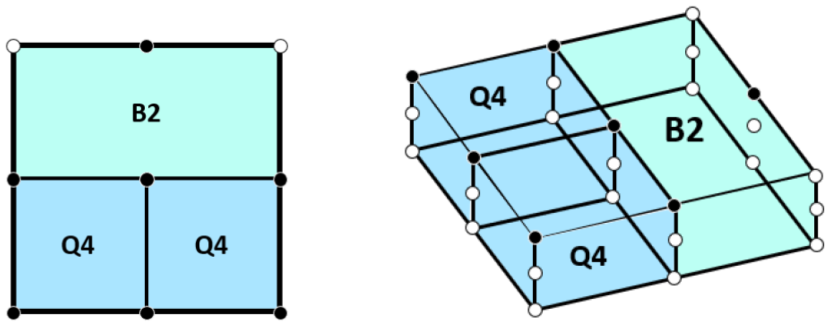

(a) 2D view (b) 3D view

Figure 1: Quarter plate: 2xQ4 1xB2 mesh

In Fig. 1 it is possible to visualize one of the described configurations: the black dots are the FEM nodes, while the white dots represent the CUF nodes added considering the thickness and the cross-section of the plate and the beam elements, respectively.

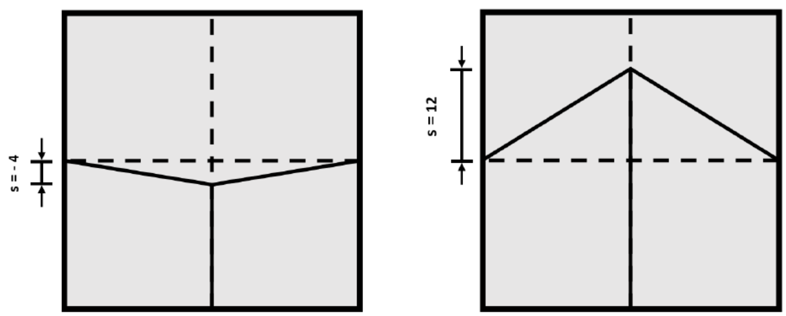

(a) Quarter plate - Parameter $s < 0$ (b) Quarter plate - Parameter $s > 0$

Figure 2: Quarter plate - mesh distortion defined by parameter 's'

The mesh distortion is characterized by the parameter s ∈ {−12,−10,−6, 0, 6, 10, 12}, which defines the coordinates of the central node of the plate quarter. Note that the parameter 's' can assume negative and positive values, as shown in Fig. 2: if the parameter s is negative, the considered element is convex; if the parameter s is positive, the element becomes non-convex.

A static analysis is performed and the results are computed in terms of transverse displacement $U_z = u_z(a, a, 0)$ (the center point on the midsurface of the entire plate) for the distorted mesh and it is normalized with respect to the reference value U_{z0} calculated for the regular mesh (s = 0). The results computed by varying the parameter s are reported in Fig. 3.

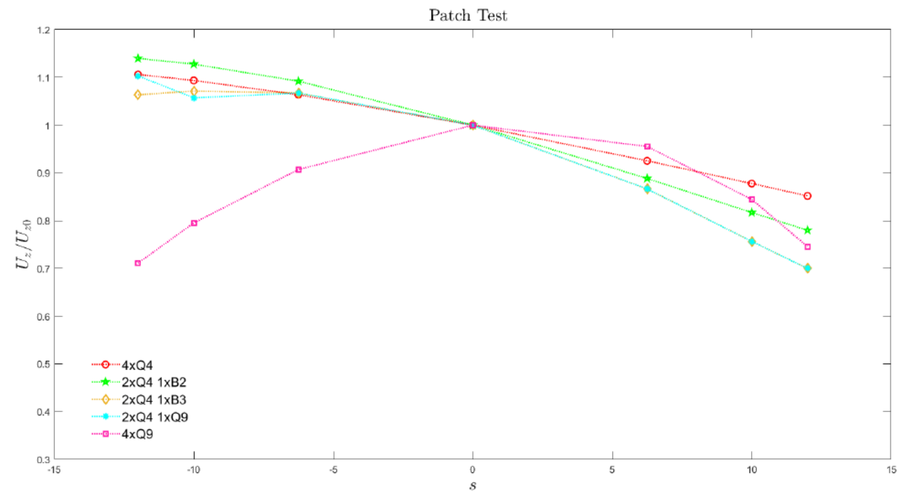

Figure 3: Variation of the ratio U_z/U_{z0} for CC quarter plate

One has to take into account that the 2x2Q9 solution is the most accurate with the highest number of degrees of freedom (DOFs=225), the 2x2Q4 (DOFs=81) is the least accurate and the other solutions are in the middle according to their related degree of approximation. The meshes 2xQ4 1xQ9 (DOFs=108) and 2xQ4 1xB3 (DOFs=108) are very similar to each other and they are compared to highlight that their solution are exactly the same, although the first uses a plate element (Q9) and the other one a beam element (B3).

Conclusions

The results demonstrate that the sensitivity to the distortion of the mixed meshes with beam elements is comparable to the regular meshes (2x2Q4 and 2x2Q9). In particular, the use of B2 beam element in the mesh 2xQ4 1xB2, with a number of DOFs equal to the mesh 2x2Q4 (DOFs=81), doesn't compromise the trend of the results when the mesh is distorted, although it permits to differentiate the number of nodes along the edges of the element (see Figure 3(a)) by reducing also the total number of the nodes in the element with respect to the other mixed meshes.

References

[1] H. Chi, L. Beirão Da Veiga, G.H. Paulino, Some basic formulations of the Virtual Element Method (VEM) for finite deformations, Comput. Methods Appl. Mech. Eng. 318 (2017) 148-192. https://doi.org/10.1016/j.cma.2016.12.020

[2] L. Beirão Da Veiga, F. Brezzi, L.D. Marini, A. Russo, The hitchhiker's guide to the virtual element method, Math. Models Methods Appl. Sci. 24:08 (2014) 1541-1573. https://doi.org/10.1142/S021820251440003X

[3] G. Li, E. Carrera, M. Cinefra, A.G. De Miguel, A. Pagani, E. Zappino, An adaptable refinement approach for shell finite element models based on node-dependent kinematics, Compos. B. Eng. 210 (2019) 1-19. https://doi.org/10.1016/j.compstruct.2018.10.111

[4] M. Cinefra, Non-conventional 1D and 2D finite elements based on CUF for the analysis of non-orthogonal geometries, Eur. J. Mech. A Solids 88 (2021) 104273. https://doi.org/10.1016/j.euromechsol.2021.104273